ELSEVIER

Journal of Molecular Catalysis A: Chemical 119 (1997) 437–447

JOURNAL OF MOLECULAR CATALYSIS A: CHEMICAL

Quantum chemical study of the electronic structure of the Ni/MoS_2 hydrodesulfurization catalysts

I.I. Zakharov *, A.N. Startsev, G.M. Zhidomirov

Boreskov Institute of Catalysis, Novosibirsk 630090, Russia

Received 21 September 1996; accepted 8 October 1996

Abstract

The role of the electronic state of the Ni atoms in the sulfide catalysts is studied by means of ab initio molecular orbital calculations. It is shown that the Ni ion with d^8 electron configuration in the square-planar sulfur surrounding is not active in the hydrodesulfurization (HDS) process. The d^8-state can be transformed to the d^6-state after adsorption of the H_2S molecule and formation of the square-pyramidal surrounding for the nickel ion. A square-pyramidal structure of the H_2S adsorption complex on Ni/MoS_2 catalysts with Ni(d^6) is calculated as the active center. The HDS catalytic cycle, for which the H_2S adsorption complex is the initial and final state, is proposed.

Keywords: Ab initio; Molecular orbital calculations; Hydrodesulfurization; Molybdenum disulfide; Hydrogen sulfide adsorption

1. Introduction

Nickel- or cobalt-promoted molybdenum sulfide catalysts are extensively studied in the hydrodesulfurization (HDS) process. Especially the role and the chemical (electronic) state of the cobalt and nickel atoms in the sulfide catalysts is a subject of numerous experimental [1–3] and theoretical [4–6] investigations. Various models for the structure of an active center (AC) of the catalyst have been proposed [1–3], but at the present the models based on the MoS_2 single slabs with Ni(Co) atoms localized in its edge plane have received the best recognition. Nevertheless, even if the similarity of the active component and MoS_2 structure does not cause any doubt, there is no unified opinion on the Ni(Co)-localization. There exist at least two points of view: a square-planar surrounding of Ni(Co) atoms with S atoms at the (1010) plane of a $MoS_2(WS_2)$ single slab [7] and a square-pyramidal surrounding of Ni(Co) with five S atoms at the edge plane of a MoS_2 single slab [8,9]. But as was shown in [3], there is no contradiction between these models: the square-planar surrounding transforms into a square-pyramidal one after adsorption of a donor molecule (Fig. 1), which was confirmed experimentally [10].

This situation is typical of pentacoordinated metal complexes. Coordination of the corresponding donor molecule to the metal in a square-planar surrounding leads to the forma-

* Corresponding author.

PII S1381-1169(96)00507-9

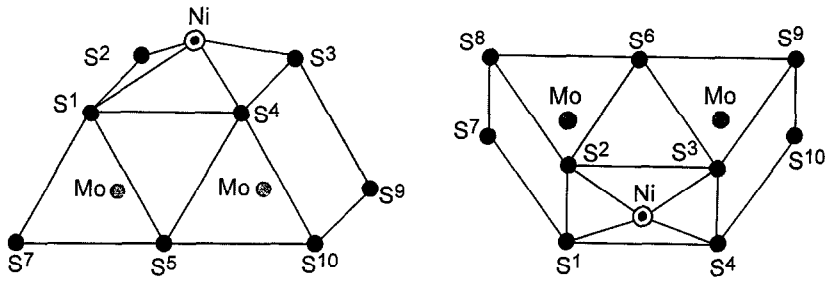

Fig. 1. Side and top view of a square-pyramidal Ni/MoS_2 active component ($NiMo_2S_{10}$-fragment).

tion of complex in which the metal is localized in a square-pyramidal environment [11,12]. The electronic state of Ni in the composition of the active component of sulfide HDS catalysts seems to be the key problem for understanding the mechanism of HDS catalysis. To our knowledge this question has not been considered in the literature thus far. We have performed ab initio calculations of $Ni(S_2C_2H_2)_2$ as a molecular model of AC in HDS catalysts. It was shown that in the square-planar coordination Ni has a d^8 electron configuration corresponding to the formal oxidation state Ni(II) [13]. In this state Ni is not active for adsorption of donor molecule as H_2S [14].

Accounting for the tendency of the $Ni(S_2C_2H_2)_2$ complex (NiBDT) to form stable dimer structures with a Ni atom transferred from a plane of the complex, one can assume [15] that there are structures for which the unusual oxidation state of Ni(W) with electron configuration d^6 can occur. Our calculations of the H_2S:NiBDT molecular adduct confirm such an assumption (Fig. 2). Two lone pairs n_σ and n_π of the H_2S molecule interact efficiently with two vacant d_σ and d_π orbitals of Ni(IV) with the electron configuration d^6 [14].

The possibility of Ni(IV) existence in the Ni/MoS_2 system may be proposed basing on the XPS data [3,16,17] giving an excess of positive charge on Ni in Ni/MoS_2 compared to NiS. The Ni(IV) oxidation state (d^6 electron configuration) is well known in the cases of octahedral fluoro $(NiF_6)^{-2}$ and dithiocarbamate $[Ni(R_2dtc)_3]^+$ complexes [18].

In this paper the ab initio calculations have been carried out for the $NiMo_2S_{10}$ cluster on the geometry suggested by Bouwens et al. [8,9].

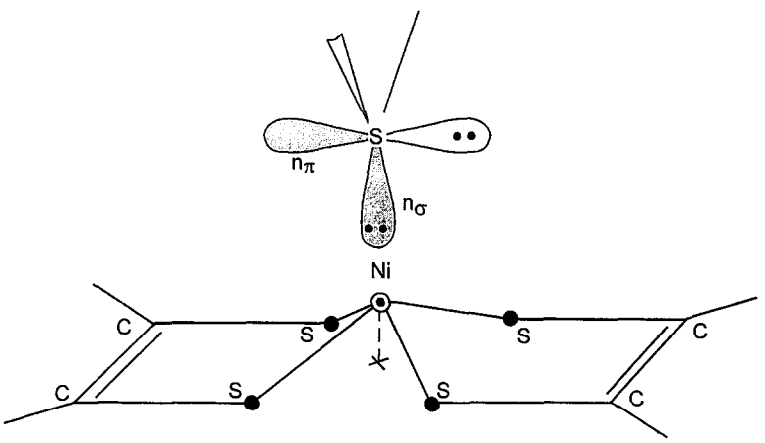

Fig. 2. Calculated adduct of H_2S molecule with chelate complex $Ni(S_2C_2H_2)_2$.

For all atoms of the cluster the charges were given according to their formal oxidation state (+2, +4 and −2 for Ni, Mo and S respectively; the possible reduction of Mo by Ni has been also taken into account [4]). We focus our attention on elucidating the electronic and energetic effects for the interaction of hydrogen sulfide (H_2S) with the active component $NiMo_2S_{10}$.

2. Method and calculation details

All calculations were carried out with use of the LANL1 effective core potential for inner shells of Ni, Mo and S atoms [19] and basis set single-ζ (MB) or double-ζ (DZ) for valence shells provided with the Gaussian 92 package [20]. The electronic correlation was taken into account using the Møller–Plesset perturbation theory at the second order (MP2) [21]. Geometry-optimized calculations for the H_2S molecule and its adsorption complex were carried out at the MP2 level with the split-valence 3-21G basis set for H atoms and LANL1DZ for the S atom. The cluster model for ab initio calculations of the active component $NiMo_2S_{10}$ has been used. At this point, we must mention a typical problem that arises when performing cluster calculations, namely, the dangling bonds and charged species. When a solid is modeled by a cluster, the terminal atoms have some orbitals that 'point to nowhere'. With this in mind [22], we calculated the cluster $NiMo_2S_{10}H_{10}$ (Fig. 3b) instead of $(NiMo_2S_{10})^{-10}$. The solid MoS_2 was considered as the fragment $(Mo_2S_{10})^{-12}$ and modeled by the cluster $Mo_2S_{10}H_{12}$ (Fig. 3a). In this model the Mo/S ratio is not stoichiometric, nevertheless, the calculated charges on Mo and S atoms are stoichiometric (Table 1) due to a chosen orbital exponent for H-'terminal' atoms. The basis set STO-3G with scale factor = 1.3 for H-'terminal' atoms, the LANL1DZ for Ni atom and the LANL1MB for S atoms were used for calculations of the clusters $Mo_2S_{10}H_{12}$ and $NiMo_2S_{10}H_{10}$. Also for the molybdenum atoms

Table 1
Calculated net charge on Mo and S atoms for the MoS_2 model cluster ($Mo_2S_{10}H_{12}$) at the Hartree–Fock (HF) and Møller–Plesset (MP2) levels

Level [a] of calculation	Mo	S^1–S^4	S^5–S^6	S^7–S^{10}	S (average)
HF	+0.88	−0.374	−0.340	−0.562	−0.44
MP2	+0.73	−0.334	−0.262	−0.489	−0.38

Length for the 'terminal' S–H-bonds calculated at the MP2 level r_e = 1.42 Å. The Mo–Mo, Mo–S and S–S bond lengths chosen are the crystallografical values for MoS_2.
[a] HF calculated energy $E = -120.33794$ a.u.; MP2 calculated energy $E = -120.80960$ a.u.

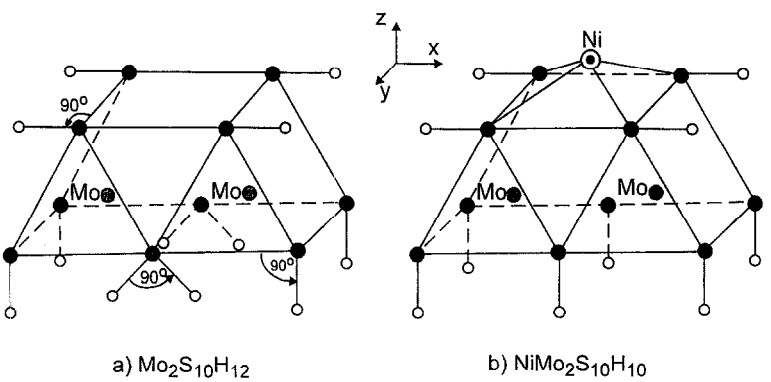

a) $Mo_2S_{10}H_{12}$ b) $NiMo_2S_{10}H_{10}$

Fig. 3. Schematic diagrams for the clusters $Mo_2S_{10}H_{12}$ and $NiMo_2S_{10}H_{10}$ with the C_{2v}-symmetry (circle with dot – Ni, grey circle – Mo, black circle – S, open circle – H).

the basis set LANL1MB was used without p-functions.

3. Electronic structure of the $NiMo_2S_{10}H_{10}$ cluster with d^8 electron configuration of Ni(II)

It is well known that the addition of Ni(Co) to $MoS_2(WS_2)$ can give rise to an enhancement of HDS activity. The effect of the Ni(Co)-promotion as an electronic (chemical) one has been supported by Harris and Chianelli [4]. This work [4] suggests that the synergetic systems behave at their surface as if they are hypothetical 'pseudo-binary' sulfides having average properties of their two components. Our (A.N.S.) study of the sulfide catalysts by modern physicochemical methods resulted in a model of the active component structure which received the name 'sulfide bimetallic species' — SBMS [3]. Considering the electronic structure of the cluster $NiMo_2S_{10}H_{10}$ as such SBMS model one can note that the calculated charge on Mo (Table 2) is smaller than for the unpromoted MoS_2 (Table 1). This is consistent with the SCF-Xα calculation result for the Co–Mo and Ni–Mo binary sulfides [4], that Mo is formally reduced relative to the Mo^{4+} presented in MoS_2. Most of the authors [1,2,4] claim that the increasing catalytic HDS activity is purely a promotion effect, while by our opinion [3], the promoter atoms are the catalysts themselves. The idea that Ni(Co) in sulfided Ni–Mo and Co–Mo catalysts is the actual catalyst rather than the promoter originates from Refs. [23–26]. That is the reason of our attention to calculation of the detail electronic structure of Ni in $NiMo_2S_{10}H_{10}$.

For the lowest energy state of $NiMo_2S_{10}H_{10}$, the electronic structure of Ni with formally empty d_{xy} level (in the coordinate system of Fig. 3) is obtained (Table 2). The calculated d_{xy} orbital population has 1.1 electrons due to coordinate-covalent bonding with the four S^1–S^4 atoms in the cluster. Such d-orbital energy level scheme looks like the square planar transition-metal complexes with one (d_{xy}) above four d-obitals, though in our case, the Ni atom is transferred from the plane of S^1–S^4 atoms by 0.48 Å (square-pyramidal coordination). The Ni basis d-functions are split into different representations in the C_{2v} point group of the cluster $NiMo_2S_{10}H_{10}$: $d_{z^2}(a_1)$, $d_{xz}(b_1)$, $d_{yz}(b_2)$, $d_{x^2-y^2}(a_1)$ and $d_{xy}(a_2)$. Calculations were performed for all the closed-shell d^N-configurations obtained from distributing the eight nickel 3d electrons among the five d-orbitals. This gives five various $^1A_1$ states for the cluster. The calculated atomic population of the d-orbitals of Ni in these states and the charge distribution of the cluster are summarized in Table 2. First of all we note that the cluster electronic states with the nickel d_{z^2}- and d_{xz}-empty orbitals are low-energy excite states, because these d-orbitals

Table 2
Calculated d^N electron configurations of divalent nickel ion (d^8) for square-pyramidal active site in the cluster $NiMo_2S_{10}H_{10}$

d^N electron configuration [a]	Calculated d-orbital electron population [b] for Ni ion [c]	Calculated net charges					MP2 energy for cluster (a.u.)
		Ni	Mo	S^1–S^4	S^5–S^6	S^7–S^{10}	
$d^8d^0_{xy}$	$d^{2.00}_{x^2-y^2}d^{2.00}_{xz}d^{2.00}_{yz}d^{2.00}_{z^2}d^{1.10}_{xy}$	+0.45	+0.54	−0.32	−0.29	−0.46	−159.24489
$d^8d^0_{z^2}$	$d^{2.00}_{xz}d^{2.00}_{yz}d^{2.04}_{xy}d^{2.00}_{x^2-y^2}d^{0.98}_{z^2}$	+0.54	+0.54	−0.36	−0.25	−0.44	−159.14497
$d^8d^0_{xz}$	$d^{2.02}_{z^2}d^{2.05}_{xy}d^{1.99}_{yz}d^{2.00}_{x^2-y^2}d^{0.80}_{xz}$	+0.65	+0.57	−0.36	−0.31	−0.44	−159.12174
$d^8d^0_{yz}$	$d^{2.04}_{z^2}d^{2.08}_{xy}d^{2.02}_{xz}d^{2.01}_{x^2-y^2}d^{0.26}_{yz}$	+0.89	+0.51	−0.43	−0.28	−0.44	−159.07642
$d^8d^0_{x^2-y^2}$	$d^{2.08}_{xy}d^{2.02}_{xz}d^{2.01}_{yz}d^{1.53}_{z^2}d^{1.03}_{x^2-y^2}$	+0.82	+0.51	−0.45	−0.32	−0.38	−159.03423

Length for the 'terminal' S–H-bond in the cluster r_e = 1.41 Å. The Ni–Mo bond length (2.80 Å) is taken from [8,9].
[a] Occupation number of nickel d orbitals in the one-determinant wavefunction used as initial approximation for the SCF calculations.
[b] Mulliken population analysis was performed on the MP2 wavefunction.
[c] The sequence of the d orbitals corresponds to that calculated for the d-splitting levels.

can realize effective σ- and π-interactions with such adsorbed molecules as hydrogen sulfide, thiophene and tetrahydrothiophene. In this paper we will concern our calculations with molecular H_2S adsorption only.

4. Structure of adsorbed H_2S complex on $NiMo_2S_{10}H_{10}$

For studying the adsorption of H_2S on the cluster $NiMo_2S_{10}H_{10}$, we have carried out calculations of electronic properties separately for the cluster (Table 2), for the free molecule H_2S and for the composite H_2S–$NiMo_2S_{10}H_{10}$ system (Fig. 4). Geometry-optimized calculations at the MP2 level for the H_2S molecule and its adsorbed complex are shown in Table 3. From the analysis of the calculated data (Tables 2 and 3) the following features are worth to mention:

(i) According to the total MP2 energy values, the $d^8d^0_{xy}$-state of Ni in the cluster represents the most stable adsorbed complex of H_2S. The corresponding MP2 energy value for the isolated $NiMo_2S_{10}H_{10}$ cluster with the same $d^8d^0_{xy}$-state of Ni (Table 2) and MP2 energy for the free molecule H_2S (Table 3) give minor bonding interaction ($E_{ads} = 36$ kJ/mol). The interaction H_2S–$NiMo_2S_{10}H_{10}$ produces very small changes of the electronic structures of the participants. The small value of the adsorption energy, 36 kJ/mol, also shows that the interaction with H_2S has a polarizative (no-covalent) nature. This is in accordance with the result

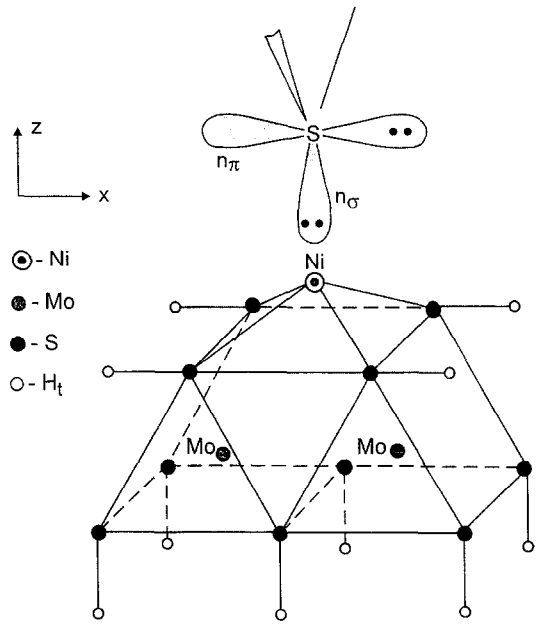

Fig. 4. Geometric structure of molecular adsorbed H_2S on a $NiMo_2S_{10}H_{10}$ cluster.

obtained by Smit and Johnson [6] that "metal–sulfur bonding is weak during adsorption". The situation is the same for $d^8d^0_{xz}$- and $d^8d^0_{yz}$-states of Ni in the H_2S adsorption complex (Table 3).

(ii) Analysis of the structure of the H_2S adsorption complex with $d^8d^0_{z^2}$- and $d^8d^0_{x^2-y^2}$-states of Ni shows that the bonding interaction is stronger than in case (i). The symmetry of the nickel d_{z^2} and $d_{x^2-y^2}$ basis functions corresponds to the same a_1 irreducible representation in the C_{2v} point group. It is clear, that these d-states of the adsorption complex are mixed,

Table 3
Calculated geometric and electronic characteristics of the H_2S adsorption complex with various d^8 electron configurations of Ni(II)

d^N-configuration of Ni	Geometric [a] and electronic characteristics of the H_2S [b] adsorption complex						MP2 energy for adsorption complex (a.u.)	E_{ads} (kJ/mol)
	Ni–S (Å)	HSH (deg)	S–H (Å)	q_{Ni}	q_S	q_H		
$d^8d^0_{xy}$	2.77	97.7	1.369	+0.40	−0.15	+0.11	−170.33702	36.0
$d^8d^0_{z^2}$	2.48	98.0	1.366	+0.46	−0.09	+0.14	−170.26686	114.3
$d^8d^0_{xz}$	3.02	96.6	1.369	+0.74	−0.15	+0.12	−170.21129	29.3
$d^8d^0_{yz}$	3.01	97.8	1.368	+0.93	−0.17	+0.11	−170.170.25	40.6
$d^8d^0_{x^2-y^2}$	2.84	98.3	1.366	+0.87	−0.16	+0.12	−170.16272	131.6

[a] Geometry of the $NiMo_2S_{10}H_{10}$ cluster was frozen with 'terminal' S–H = 1.41 Å.
[b] MP2/LANL1 calculation for the free H_2S molecule: $E = -11.07840$ a.u.; SH = 1.371 Å, HSH = 95.12°, $q_S = -0.148$, $q_H = +0.074$.

although the interaction of the σ-lone pair of H_2S with the d_{z^2}-orbital only can be understood in the terms of overlap. Both of these states of the H_2S adsorption complex are excite-energy states and will be unstable in real surface phenomena.

5. Electronic structure of the clusters with d^6 electron configuration of Ni(IV)

The common chemistry of nickel is the chemistry of the +2 oxidation state, although its known chemistry spans all oxidation states from −1 to +4 [17]. The nickel(II) ion has a d^8 electron configuration and, with weak-field ligands such as H_2O, it forms a six-coordinated ion with octahedral symmetry and a paramagnetic ($t_{2g}^6 e_g^1 e_g^1$) ground state. The splitting of the d orbitals shows two d_σ above three d_π orbitals. The thermodynamic stability of the six-coordinate complexes generally increases as the ligand-field strength increases. A strong square-planar ligand field results in formation of the diamagnetic ground state with one (d_{xy}) above four d orbitals. Nickel(IV) chemistry is commencing some 90 years after the synthesis of the heteropoly(molybdate) $[NiMo_9O_{32}]^{6-}$ complex [27]. In the case of nickel in a high oxidation state, it is imperative that the ligands should have more negative charges. In other words, the number of ligands and its electronegativity should be high. In this way the model of pseudooctahedral-coordinated Ni(IV) with a d^6 electron configuration can be understood. Strong metal–ligand bonds here mean unstable e_g^*-levels which in Ni(II) are doubly occupied. Facile loss of e_g^* electrons can then give Ni(IV) species (Fig. 5). Actually, nickel(IV) complexes are diamagnetic and have a strong preference for an octahedral geometry [28,29] with $10Dq = 20000\ cm^{-1}$ [30] greater than for Ni(II) ($10Dq$ 7250 cm^{-1} [31]), for NiF_6^{2-} and NiF_6^{4-}, respectively.

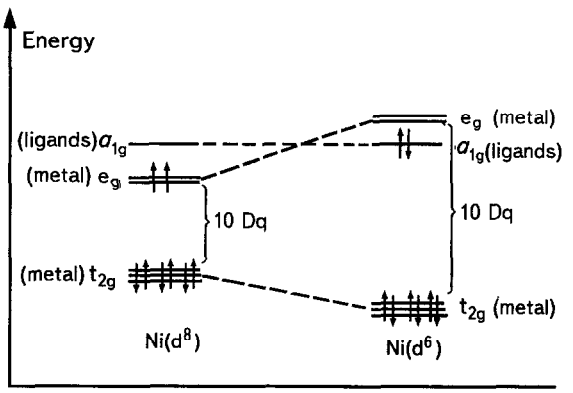

Fig. 5. Correlation diagram for the frontier molecular orbitals of octahedral Ni-complexes with d^8 and d^6 electron configuration.

The +IV oxidation state for the nickel triad elements (Ni, Pd, Pt) provides a firmer basis for proposals involving this species in catalysis [32]. In the case of HDS reaction, Ni(IV) cation formation is expected to enhance the nucleophilic attack for such donor molecules as hydrogen sulfide, thiophene and tetrahydrothiophene. On the other hand, an electron-deficient metal atom on the surface should have a very high resistance to sulfur poisoning. As is shown in [33], the rate of deactivation of a Pd/Al_2O_3 catalyst by thiophene during ethylbenzene hydrogenation decreases as the concentration of $Pd^{\delta+}$ increases [34].

Table 4
Calculated electronic structures of the cluster $NiMo_2S_{10}H_{10}$ and the H_2S adsorption complex with d^6 electron configuration of Ni(IV)

Molecular cluster	Calculated d-orbital electron population for Ni ion	Geometry [a] of H_2S adsorption complex			MP2 energy (a.u.)
		Ni–S (Å)	HSH (deg)	S–H (Å)	
$NiMo_2S_{10}H_{10}$	$d_{xy}^{2.03} d_{x^2-y^2}^{1.95} d_{yz}^{1.97} d_{xz}^{1.14} d_{z^2}^{1.37}$	—	—	—	159.46084
H_2S [b] adsorption complex	$d_{xy}^{2.02} d_{x^2-y^2}^{1.98} d_{yz}^{1.99} d_{xz}^{1.67} d_{z^2}^{1.63}$	2.60	102.0	1.36	−170.57075

[a] Geometry of the cluster $NiMo_2S_{10}H_{10}$ was frozen with 'terminal' S–H = 1.41 Å.
[b] Calculated adsorption energy E_{ads} = 82.8 kJ/mol.

The possibility of formation Ni(IV) with d^6 electron configuration in the cluster $NiMo_2S_{10}H_{10}$ and in the H_2S adsorption complex is demonstrated by ab initio calculations and shown in Table 4. We will discuss these results on the basis of comparison with the lowest energy state for divalent Ni ($d^8d^0_{xy}$) in the cluster $NiMo_2S_{10}H_{10}$ (Table 2) and in the H_2S adsorption complex (Table 3). First of all, computed MP2 total energies for the cluster and the adsorption complex with Ni(IV), $d^6d^0_{z^2}d^0_{xz}$ electron configuration are lower than for divalent Ni(II), $d^8d^0_{xy}$ ($\Delta E_1 = 5.9$ eV and $\Delta E_2 = 6.4$ eV, respectively, see Tables 2–4). The adsorption energy of the H_2S molecule for Ni(IV), d^6-state ($E_{ads} = 82.6$ kJ/mol) is greater than for Ni(II), d^8-state ($E_{ads} = 36.0$ kJ/mol). The calculated equilibrium bond distances Ni–SH_2 are 2.60 Å and 2.77 Å for Ni(IV) and Ni(II), respectively. From this, the adsorption energy appears to increase with increases in the formal oxidation state of Ni in the cluster. Because the stabilization energy of the d^6-state for the H_2S adsorption complex ($\Delta E_2 = 6.4$ eV) is greater than for the free cluster ($\Delta E_1 = 5.9$ eV), we can conclude that the d^6-state of the Ni(IV) ion is stabilized during adsorption. The relatively strong interaction between the H_2S and the Ni(IV) ion can be understood in terms of orbital overlap (see Scheme 1). Two lone pairs n_σ and n_π of the H_2S molecule interact efficiently with two vacant $d_\sigma(z^2)$ and $d_\pi(xz)$ orbitals of Ni(IV), d^6 electron configuration. It is interesting to note that there is a difference in such interaction between the Ni(IV) ion and metallic

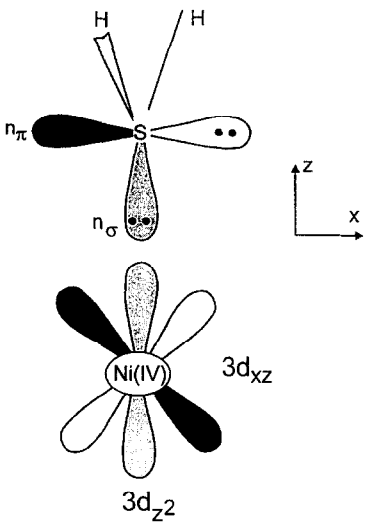

Scheme 1. Scheme for $n_\sigma - 3d_{z^2}$ and $n_\pi - 3d_{xz}$ orbital interactions of hydrogen sulfide with the Ni(IV)ion.

nickel on the surface. The latter results in the 'tilted' geometry of H_2S adsorbed with competition between σ- and π-lone pairs for the maximum bonding to the surface [35]. The charge transfer from H_2S to the cluster $NiMo_2S_{10}H_{10}$ due to adsorption and the charge transformation of cluster due to the Ni(II) → Ni(IV) transition are demonstrated in Table 5. Changes in the values of the charge of S^1–S^4 atoms in the cluster are the most dramatical due to Ni(IV) formation. Increase in the formal charge of nickel ($Ni^{2+} \rightarrow Ni^{4+}$) in the cluster has brought about twice changes in the calculated charge on the Ni atom (Table 5).

The second point to consider is the change in the Mo oxidation state. Fig. 6 shows a proposed surface reconstruction of the (1010) edge of a

Table 5
Calculated net charges of the cluster $NiMo_2S_{10}H_{10}$ and the H_2S adsorption complex for Ni(II) and Ni(IV) ions

Molecular cluster	d^N configuration of Ni	Calculated net charges						
		Ni	Mo	S^1–S^4	S^5–S^6	S^7–S^{10}	S	H
$NiMo_2S_{10}H_{10}$	$d^8d^0_{xy}$ Ni(II)	+0.45	+0.54	−0.32	−0.29	−0.46	—	—
	$d^6d^0_{z^2}d^0_{xz}$ Ni(IV)	+0.98	+0.60	−0.46	−0.31	−0.44	—	—
H_2S [a] adsorption complex	$d^8d^0_{xy}$ Ni(II)	+0.40	+0.55	−0.33	−0.27	−0.44	−0.15	+0.11
	$d^6d^0_{z^2}d^0_{xz}$ Ni(IV)	+0.97	+0.58	−0.46	−0.30	−0.45	−0.18	+0.16

[a] Calculated net charges for free H_2S molecule: $q_S = -0.148$; $q_H = +0.074$.

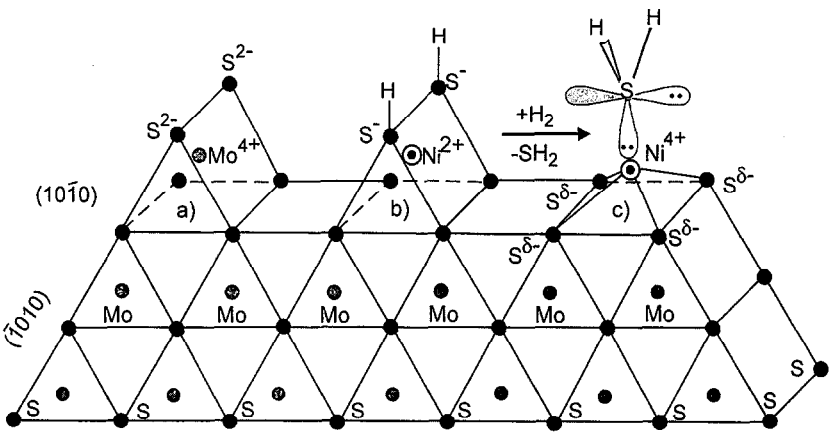

Fig. 6. Top-view of the reconstructed of the (1010) edge plane of a single slab of MoS_2; grey circle – Mo atoms, circle with dot – Ni atoms, black circle – S atoms. (a) six-fold coordinated Mo^{4+} in the trigonal sulfur prims of the MoS_2 unit cell; (b) six-fold coordinated Ni^{2+} (two ligands are actually SH-groups, because of charge neutrality, when replacing a Mo^{4+} by a Ni^{2+} cation); (c) a square-pyramidal structure of a Ni^{4+}-active site.

single slab of MoS_2. Six-coordinated Mo^{4+} ions are in the trigonal sulfur prism of the MoS_2 unit cell ('bulk-like' position) (Fig. 6a). The IR study of the adsorption of NO on Ni–Mo catalyst by Topsoe and Topsoe [36] indicated that the edge Mo atoms are screened and cannot be directly responsible for the catalysis. As Fig. 6b demonstrates, the Ni^{2+} ion is attached to the square face of a trigonal sulfur prism, but to obtain electrical neutrality two of six ligands should be SH^- groups (in place of S^{2-}). As shown in [8,9], the Ni(Co) atoms at the edges of a single slab of MoS_2 have a distorted 5- to 6-fold sulfur coordination (Ni–S coordination number is equal to 5.3). This can be related to our result on stabilization of Ni(IV) ions at the edges of MoS_2. A square-pyramidal structure of the H_2S adsorption complex on Ni/MoS_2 catalyst with Ni(IV), d^6 can be proposed as the active center in the HDS process (Fig. 6c). From a purely chemical point of view, when the sulfur atom is removed as H_2S from MoS_2 molybdenum reduction must be expected [37]. The change of the Mo oxidation state (reduction) must occur due to nickel oxidation also ($Ni^{2+} \rightarrow Ni^{4+}$) (see Fig. 6, reaction b → c.) Nevertheless, our results do not confirm these expectations, as can be seen comparing Tables 1 and 5. The calculated MP2 values of charges on Mo atoms in MoS_2 ($q = +0.73$) and in Ni/MoS_2 ($q = +0.60$) indicate, that the significant reduction of Mo does not occur. The main changes in calculated charges are realized on S^1–S^4 and Ni atoms of the surface cluster (Table 5). The oxidation of nickel ($Ni^{2+} \rightarrow Ni^{4+}$) results in significant changes of the charges on Ni atom ($+0.45 \rightarrow +0.98$). These are in accordance with the XPS data [15]:

(i) The Mo 3d line in XP-spectra of the sulfide Mo/Al_2O_3 catalysts is characterized by well-resolved doublets with BE Mo $3d_{5/2} = 229.0 + 0.2$ eV, which corresponds to bulk MoS_2, and does not change in bimetallic sulfide $[Ni(Co)–Mo]/Al_2O_3$ catalysts.

(ii) The S 2p line in all the catalysts studied exhibits a broad maximum with BE = 162.0 + 0.3 eV. No regularities in its position is found for the mono- and bimetallic sulfide catalysts.

(iii) The Ni $2p_{3/2}$ and Co $2p_{3/2}$ lines in the sulfide [Ni(Co)–Mo] catalysts are shifted towards high values of BE's by 1.0 (0.5) eV correspondingly in comparison with the sulfide $Ni(Co)/Al_2O_3$ catalysts.

A possible explanation in increase of the Ni oxidation state in the process of the catalyst sulfurization under hydrogen atmosphere seems to be as follows. Formally, reaction b → c presented in Fig. 6, should be considered as reduc-

tive elimination, but we believe that under the catalysts preparation conditions the reaction of the oxidative addition of the hydrogen molecule occurs. This reaction of oxidative addition of H_2 to the square-planar Ir(I) complex was discovered over 30 years ago [40] and nowadays it is one of the key reactions in homogeneous catalysis by the VIII group metal complexes [41,42]. As was underlined in [41], the square-planar complexes with d^8 electron configuration have a strong tendency to the oxidative hydrogen addition resulted in the transition metal atom with d^6 electron configuration. As also well known, this reaction is the first step of the active center formation in the Wilkinson olefin hydrogenation catalysts [43]. Besides, η-H_2 transition metal complexes are synthesized [44] and well characterized [45] and now they are considered as precursors into the oxidative addition reactions. Molecular hydrogen complexes represent a relatively new but rapidly expanding area of transition metal chemistry [46,47]. Based on these investigations we believe that the high oxidation state of Ni into the active centers of the HDS catalysts resulted from the oxidative addition of H_2 under conditions of catalyst preparations. This problem is a subject of our current investigation.

6. Catalytic cycle and concerted mechanism of thiophene hydrogenolysis

Fig. 7 shows a proposed catalytic cycle for HDS of thiophene over Ni(IV)/MoS_2 structure. The thiophene hydrogenolysis reaction occurs on SBMS of any composition with low activation energy (30–60 kJ/mol) and high selectivity. The reaction involves 1 molecule of thiophene and 3 (or 4) molecules of hydrogen without appearance of the intermediate products in a gas phase. The following mechanism may be proposed [3]:

Adsorption of a thiophene molecule is performed on an active Ni(d^6) site replacing a H_2S molecule. The small calculated value of E_{ads}

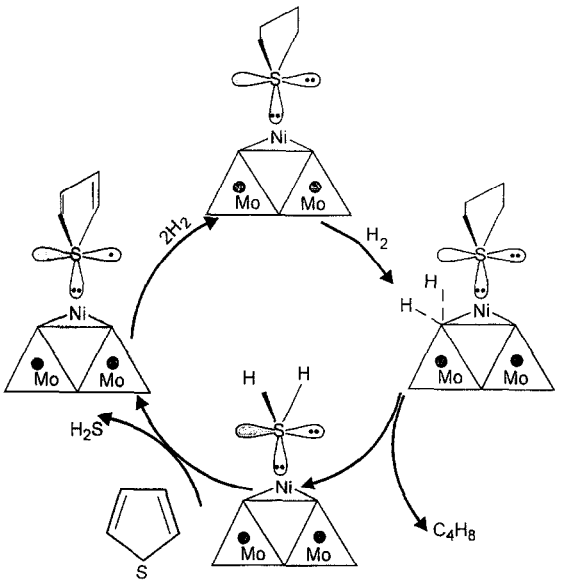

Fig. 7. Proposal for thiophene HDS catalytic cycle over Ni(IV)/MoS_2.

confirm the essential reversibility of H_2S adsorption in the reaction conditions and the possibility of adsorbed H_2S being supplanted by thiophene. Hydrogenation of the thiophene molecule results in the destruction of the π-system of the aromatic ring and an additional lone pair appears on the S atom of the tetrahydrothiophene (THT). Because THT is more basic than thiophene, it does not desorb into the gas phase. The calculated [38] heat of adsorption in the series H_2S < thiophene < THT correlates with present concept. Electron density from the S atom of THT is transferred to catalysts and localized on the its terminal S atoms, which is a driving force for the dissociative adsorption of dihydrogen. Thereupon activated hydrogen is transferred to the adsorbed THT molecule and the process is accomplished with C–S bond scission and butene desorption into the gas phase (Fig. 7). We would like to stress, that the H_2S adsorbed complex is regarded as the initial and final step in the HDS mechanism. So, the proposed mechanism does not contradict to the one suggested previously [3], but makes it more detailed. Recently the catalytic cycle for HDS of thiophene over Co–Mo catalysts was pro-

posed [39], where the Co atom is an active center for C–S bond homolysis.

7. Conclusions

On the basis of the calculations presented here, we consider that the Ni(d^8) ion in the square-planar sulfur surrounding, which can be realized in real catalysts [7], is not active in the HDS process, but the d^8-state can transform to the d^6-state in the square-pyramidal surrounding of Ni. After adsorption of the H_2S molecule, its two n_σ and n_π lone pairs efficiently interact with two vacant d_σ- and d_π-orbitals of Ni(d^6) and stabilize the active state of the sulfide bimetallic species (SBMS) — the active component of the HDS catalysts. Therefore, we believe that this H_2S adsorption complex is the initial and final step of the catalytic cycle.

Acknowledgements

The authors are grateful to I.V. Yudanov and Dr. D.I. Kochubey for helpful discussions.

References

[1] H. Topsoe and B.S. Clausen, Catal. Rev. Sci. Eng. 26 (1984) 395.
[2] R. Prins, V.H.J. de Beer and G.A. Somorjai, Catal. Rev. Sci. Eng. 31 (1989) 1.
[3] A.N. Startsev, Catal. Rev. Sci. Eng. 37 (1995) 353.
[4] S. Harris and R.R. Chianelli, J. Catal. 98 (1986) 17.
[5] M. Neurock and R.A. van Santen, J. Am. Chem. Soc. 116 (1994) 4427.
[6] T.S. Smit and K.H. Johnson, J. Mol. Catal. 91 (1994) 207.
[7] D.I. Kochubey, M.A. Kozlov, K.I. Zamaraev, V.A. Burmistrov, A.N. Startsev and Yu.I. Yermakov, Appl. Catal. 14 (1985) 1.
[8] S.M.A.M. Bouwens, D.C. Koningsberger, V.H.J. de Beer, S.P.A. Louwers and R. Prins, Catal. Lett. 5 (1990) 273.
[9] S.M.A.M. Bouwens, J.A.R. van Veen, D.C. Koningsberger, V.H.J. de Beer and R. Prins, J. Phys. Chem. 95 (1991) 123.
[10] W. Nieman, B.S. Clausen and H. Topsoe, Catal. Lett. 4 (1990) 355.
[11] R.R. Holmes, Progr. Inorg. Chem. 32 (1984) 119.
[12] R. Eisenberg, Progr. Inorg. Chem. 12 (1970) 295.
[13] I.V. Yudanov, I.I. Zakharov, A.N. Startsev and G.M. Zhidomirov, Zh. Strukt. Khim. 37 (1996) N2 (Engl. transl.).
[14] I.V. Yudanov, I.I. Zakharov, A.N. Startsev and G.M. Zhidomirov, React. Kinet. Catal. Lett. 60 (1997).
[15] S. Alvarez, R. Vicente and R. Hoffman, J. Am. Chem. Soc. 107 (1985) 6253.
[16] A.N. Startsev and A.V. Kalinkin, Kinet. Catal. 35 (1994) 267 (Engl. trans.).
[17] A.P. Shepelin, P.A. Zhdan, V.A. Burmistrov, A.N. Startsev and Yu.I. Yermakov, Appl. Catal. 11 (1984) 29.
[18] K. Nag and A. Chakravorty, Coord. Chem. Rev. 33 (1980) 87.
[19] P.J. Hay and W.R. Wadt, J. Chem. Phys. 82 (1985) 270, 299; W.R. Wadt and P.J. Hay, J. Chem. Phys. 82 (1985) 284.
[20] M.J. Frisch, G.W. Trucks, H.B. Schlegel, P.M.W. Gill, B.G. Johnson, M.W. Wong, J.B. Foresman, M.A. Robb, M. Head-Gordon, E.S. Replogle, R. Gomperts, J.L. Andres, K. Raghavachari, J.S. Binkley, C. Gonzalez, R.L. Martin, D.J. Fox, D.J. DeFrees, J. Baker, J.J.P. Stewart and J.A. Pople, Gaussian 92/DFT, Revision G.2 (Gaussian, Inc., Pittsburgh, PA, 1993).
[21] J.S. Binkley and J.A. Pople, Int. J. Quant. Chem. 9 (1975) 229.
[22] G.M. Zhidomirov and V.B. Kazansky, Adv. Catal. 34 (1986) 131.
[23] J.C. Duchet, E.M. van Oers, V.J.H. de Beer and R. Prins, J. Catal. 80 (1983) 386.
[24] Yu.I. Yermakov, V.A. Burmistrov and A.N. Startsev, Appl. Catal. 11 (1984) 1.
[25] J.P.R. Vissers, V.H.J. de Beer and R. Prins, J. Chem. Soc. Faraday Trans. I 83 (1987) 2145.
[26] A.N. Startsev, V.A. Burmistrov and Yu.I. Yermakov, Appl. Catal. 45 (1988) 191.
[27] R.D. Hall, J. Am. Chem. Soc. 29 (1907) 692.
[28] G. Foulds, Coord. Chem. Rev. 80 (1987) 1.
[29] A.G. Lappin and A. McAuley, Adv. Inorg. Chem. 32 (1988) 241.
[30] G.C. Allen and K.D. Warren, Inorg. Chem. 8 (1969) 753.
[31] K. Khox, R.G. Shulman and S. Sugano, Phys. Rev. 130 (1963) 512.
[32] A.J. Canty, Platinum Metals Rev. 37 (1993) 2.
[33] X.L. Seoane, P.C.L'Argentiere, N.S. Figoli and A. Arcoya, Catal. Lett. 16 (1992) 137.
[34] A. Arcoya, X.L. Seoane, N.S. Figoli and P.C.L'Argentiere, Appl. Catal. 62 (1990) 35.
[35] I.I. Zakharov, V.I. Avdeev and G.M. Zhidomirov, Surf. Sci. 277 (1992) 407.
[36] N.-Y. Topsoe and H. Topsoe, J. Catal. 84 (1983) 386.
[37] R.P. Diez and A.H. Jubert, J. Mol. Catal. 73 (1992) 65.
[38] N.N. Bulgakov and A.N. Startsev, Mendeleev Commun. 1 (1991) 97.
[39] H. Topsoe, B.S. Clausen, N.-Y. Topsoe, J.K. Norskov, C.V. Oveesen and C.J.H. Jacobsen, Bull. Soc. Chim. Belg. 104 (1995) 283.
[40] L. Vaska and J.W. DiLuzio, J. Am. Chem. Soc. 84 (1962) 679.
[41] G. Henrici-Olive and S. Olive, The Chemistry of the Catalyzed Hydrogenation of Carbon Monoxide, Springer-Verlag, Berlin, Heidelberg, 1984, ch. 5.

[42] M.L. Bender, Mechanism of Homogeneous Catalysis from Proton to Proteins, Wiley-Interscience, New York, London, Sydney, Toronto, 1971, ch. 8.
[43] J. Halpern, T. Okamoto and A. Zachariev, J. Mol. Catal. 2 (1976) 65.
[44] G.J. Kubas, R.R. Ryan, B.I. Swanson, P.J. Vergamini and J.J. Wasserman, J. Am. Chem. Soc. 106 (1984) 451.
[45] Z.W. Li and M.B. Taube, J. Am. Chem. Soc. 113 (1991) 8946.
[46] D.M. Heinekey and W.J. Oldham, Chem. Rev. 93 (1993) 913.
[47] P.G. Jesson and R.H. Morris, Coor. Chem. Rev. 121 (1992) 155.